EE 412 2014 Spring Quarter Final Report

Molecular Vapor Deposition and Patterning of Organosilane Self-Assembled Monolayers for Directed Growth of Neuron Cells.

Felix Alfonso & Hsin-Ya Lou
Mentor : Michelle Rincon & J Provine

Introduction

The development of micropatterning methods for biotechnology applications has inspired designs of smarter biocompatible surfaces. Investigation of the surface properties and their interaction with living organism are essential for the application of these materials toward microsystems, tissue engineering, electrochemical systems (MEMS) and biosensors.[1, 2] In order to facilitate the integration of solid state devices and biological materials extensive focus has been given to organic thin films as a mediator. Self-assembled monolayers (SAMs) are organic molecules that spontaneously assembled onto a surface by adsorption and form ordered structures. They consist of a surface reactive group which covalently binds to the substrate, a hydrocarbon spacer, and a functional group that tailor the surface properties. Modification of the spacer and free chemical group provides control of the physical and chemical properties of the surface: wetting, adhesive, electronic, sensoring, catalytic and biomolecular anchoring.[3-6]

The two most common types of SAMs are alkanethiol and organosilane.[7] Alkanethiol form a semi-covalent bond on the gold surfaces while organosilanes form covalent bonds with metal oxides surfaces following nucleophilic substitution by surface hydroxyl groups. Alkanethiol monolayers on planar Au surfaces undergo oxidation upon prolonged exposure to air which severely limits long time use.[8] On the other hand, organosilane mechanical and chemical stability in ambient environment once they have been anchored to a surface makes them great candidate for biomedical solid-state devices. Microcontact printing, photolithography, scanning probe lithography, electron-beam lithography, and ink-jet printing are common patterning techniques used for directed growth of cells.[7] SAMs versatility and compatibility with various patterning techniques makes it suitable for cell patterning.

A key concern mentioned numerous times in literature is the reproducibility and coverage of these organic films. The organic films can be deposited onto the substrate by solution phase deposition and/or chemical vapor deposition. Solution phase deposition is one of the most studied methods; however, it often produces irreproducible and poor quality films due to the self-polymerization of the precursor.[9, 10] Hence, attention has been directed toward chemical vapor deposition as the prefer method to obtained high density and uniform films. Molecular vapor deposition (MVD) is a powerful technique for fabrication of high quality organic films with conformal coating on high surface substrates.[11-15] Similarly to atomic layer deposition (ALD), the precursor is introduced to the chamber under vacuum via pulses. The self-limiting process occurs and the excess is evacuated from the reaction chamber. This process allows great control over the film growth and uniformity.

The complexity of natural neural networks makes it difficult to study the development, activity, and dynamics in vivo of the action potential. The solution is to create a simplify neural network models in vitro based on patterned SAMs surface with promoting and suppressing functional groups for directed growth of the neurons. Liu et al. have used silane substrate N-1[3-(trimethoxysilyl) propyl) diethylenetriamine (DETA) for grow and patterning of cells. They investigated the immunocytochemical and electrophysiological properties of the sensory neurons on DETA. Yamamoto et al. fabricated patterned DETA and octadecyltrimethoxysilane (ODS) SAMs on a Pyrex glass slide to serve as a template to array primary neurons. DETA and ODS worked as a promoter and suppressor of growth, respectively. Using wet femtosecond-laser, the neurites were guided to create artificial neuronal circuits. Applying the previous work, neurons cells can be grown on modify electrodes to study the electrical activities of neural networks.

Herein, we report an evaluation of the recipes used to deposit DETA and ODS using the MVD process on silicon and Pyrex wafers. Furthermore, the surfaces were patterned using photolithography. To measure the quality of the films contact angle measurement were taken and analyzed for both DETA and ODS. Taking advantage of the primary amine group in DETA, fluorescein isothiocyanate (FITC) was conjugated to the SAMs and fluorescent spectroscopy was used to characterize the uniformity of the deposition.

Results

Recipe of deposition

1. Preheat

During the preheat process, every part of MVD is heated to specific temperature that written in the recipe. In the research, we set the temperature of reaction chamber to 150°C which is normal condition.[12,17,18] The temperatures of ODS and DETA chambers are set to be lower than reaction chamber to prevent condensation of organosilane vapor when entering into the reaction chamber.

1	Flow (N_2)		20	sccm
2	Heater	6 (Trap/Pump line)	130	Deg C
3	Heater	7 (Stop valve)	150	Deg C
4	Heater	8 (Reaction Chamber)	150	Deg C
5	Heater	9 (Reaction Chamber)	150	Deg C
6	Heater	13 (ODS)	100	Deg C
7	Heater	14 (DETA)	100	Deg C
8	Stabilize	6		
9	Stabilize	7		
10	Stabilize	8		
11	Stabilize	9		
12	Stabilize	13		
13	Stabilize	14		
14	Wait		600	sec

2. Chamber Purging

Before organosilane vapor enter into the reaction chamber, the chamber need to be purged with nitrogen gas several times to remove any water vapor inside the chamber. The removal of water vapor prevents the hydroxylation of organosilane prior to attaching to the surface.

15	Stopvalve		0 (Close)	
16	Wait		60	sec
17	Stopvalve		1 (Open)	
18	Wait		60	sec
19	Goto	16	3	

3. Reaction

When the reaction start, Stopvalve of the vacuum will close and the chamber with organosilane will open to let organosilane vapor enters into the reaction chamber, which terms "pulse". We set the pulse to be 30 seconds to ensure that the vapor enters into the chamber till the pressure reach equilibrium, and the reaction starts. After the reaction, the Stopvalve will open to remove all of the free organosilane. In this research, we will adjust reaction time (step 25) and number of pulses (step 27) to optimize the deposition efficiency.

20	Flow (N_2)		0	sccm
21	Wait		20	sec
22	Stopvalve		0	
23	Wait		0.5	sec
24	Pulse	3 (3 for ODS, 4 for DETA)	30	sec
25	Wait		3600	sec
26	Stopvalve		1	
27	Goto	21	2	
28	Wait		240	sec
29	Flow (N_2)		20	sccm

Optimization of ODS deposition

We first demonstrated that the surface cleanness could be quantified by the contact angles. Small drops of water were put on dirty silicon wafers and oxygen plasma treated wafers. It was showed that the contact angles decreased significantly after plasma cleaning, indicating that the surface was totally cleaned of organic residues and thus became highly hydrophilic (Fig. 1).

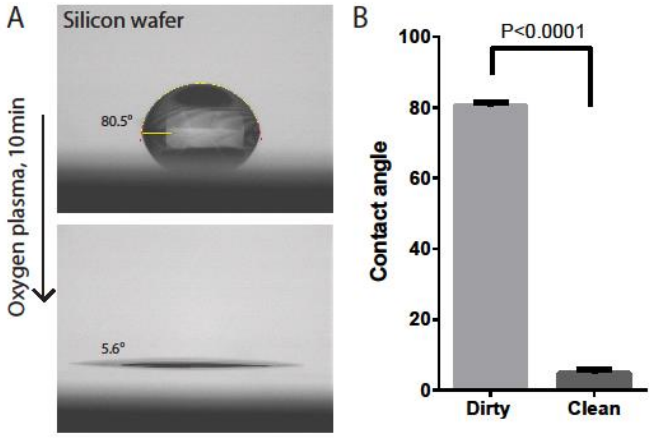

Figure 1: Relation between surface cleanness and contact angle. (A) Small drops of water on both dirty and clean silicon wafer. (B) The contact angle of dirty wafer is significantly bigger than plasma-cleaned wafer.

In the research both Pyrex and silicon wafer were used for studying organosilane deposition. The Pyrex wafers are composed of multiple oxide including SiO_2, Na_2O, K_2O, and B_2O_3 while silicon wafers are pure Si crystal. Thus, we first need to study the relation between surface compositions and ODS deposition efficiency. Both Pyrex and silicon wafers were deposited with ODS in 150°C for either 60 minutes or 120 minutes, and the results showed that the contact angles were similar for different wafers with the same deposition time (Fig. 2A). However, same type of wafers with different deposition times gave different contact angles. This indicated that the ODS deposition efficiency depends on deposition time but surface composition (Fig. 2B). In addition, regardless of the time of the reaction, the expected contact angle for ODS was not reached which was 110°. [3, 17, 18]

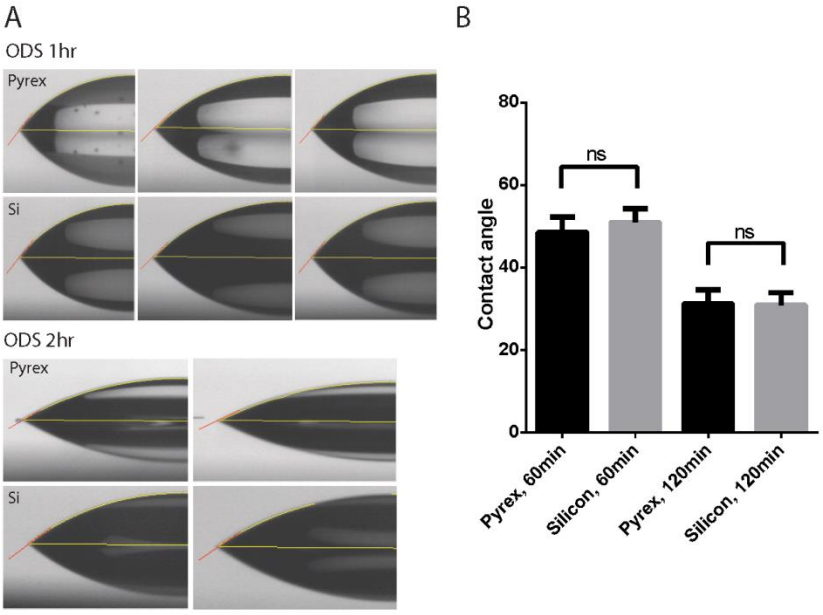

Figure 2: ODS deposition on silicon and Pyrex wafers (A) Small drops of water on Pyrex wafers and silicon wafers with different OTMS deposition times. (B) The contact angles of silicon and Pyrex wafers with the same deposition times were similar (P>0.05). However, contact angles changed with different deposition times.

Next, we tried to find the deposition time for best deposition efficiency. We assumed that longer deposition could result in higher deposition efficiency. We tested depositing ODS with different time periods from 10 minutes to 6 hours in 150°C on silicon wafers. It was found that the contact

angle increased with reaction time and decreased when reaction time was longer than 1 hour. However, the two hour and six hour deposition showed almost no difference (Fig. 3). As a result, we concluded that 1 hour is the best reaction period for ODS deposition.

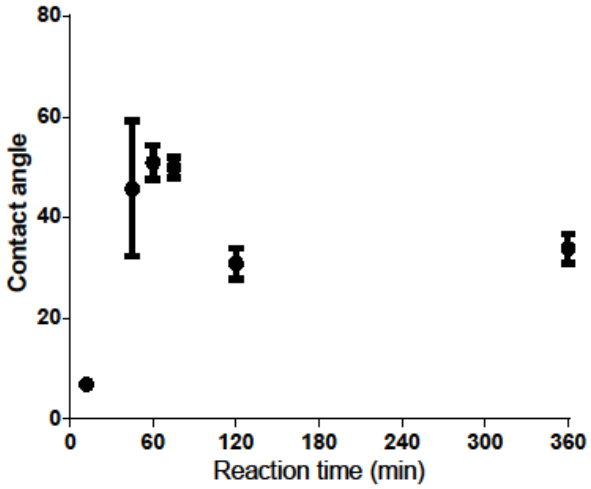

Figure 3: Contact angles of silicon wafers increased with increasing ODS deposition time, but decreased once the reaction time was longer than 1 hour. The value reached to equilibrium when the reaction time went to 6 hours.

In addition to deposition time, different factors were also been studied. First, we tested same deposition time with different number of ODS pulses. The results showed that contact angle increased with increasing number of pulses (Fig. 4A). Since every pulse will replace the reaction chamber with fresh ODS vapor, it was suggested that more ODS pulses could increase deposition efficiency, and thus increase the contact angle. However, when increase total deposition time with 12 pulses per hour, the contact angle didn't have significantly increasing (Fig. 4B). Also, we deposited ODS with different temperatures and found that lower temperature result in higher contact angle (Fig. 4C). In conclusion, deposition with multiple pulses and lower temperature could increase ODS deposition efficiency.

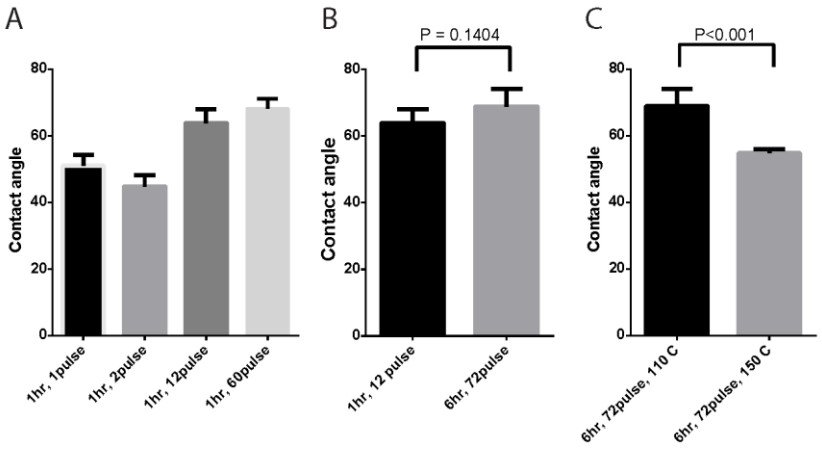

Figure 4: (A) With same deposition time, increasing number of pulses will increase deposition efficiency. (B) With the same frequency of pulses, increase deposition time from 1 to 6 hours could only increase contact angle to about 5 degrees. (C) When decreased the temperature of reaction chamber, the contact angle also decreased.

Optimization of DETA deposition

The recipe of DETA deposition is the same as the ODS deposition. When measuring contact angle of wafers with DETA deposited, it was found that when changing deposition time or pulse frequency, the contact angles changed less compared with ODS (Fig. 5). The contact angle for DETA after liquid-phase deposition is 40°; however, gas phase deposition resulted in a smaller contact angle.[19] With three amino groups, DETA is more hydrophilic than ODS. Thus, contact angle changed less with increasing DETA deposition efficiency because the surface could still maintain hydrophilic. To evaluate the DETA deposition, we use fluorescein isothiocyanate (FITC), a derivative of fluorescein which contains isothiocyanate group which could react with amino group of DETA to covalently bind on the surface (Fig. 6A). After DETA deposition, the wafer was incubated in ethanol solution with 5mg/mL FITC over 24 hours at room temperature. Than the wafer was rinsed with clean ethanol to remove free FITC and dried by nitrogen flow. The florescence was imaged by epi-fluorescence microscopy using blue light. The excitation and emission spectrum peak of are nearly 495 and 519nm, respectively. The florescence images showed that 2-hour-long DETA deposition gave higher florescence intensity than 1-hour-long DETA deposition, which related to better deposition efficiency (Fig 6B).

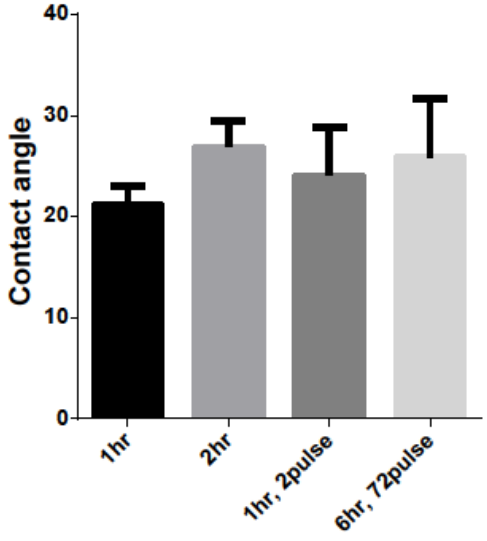

Figure 5: The contact angles of DETA deposition on silicon wafers. One-hour deposition resulted in 20 degree of contact angle, while two-hour deposition gave 30 degree. Compared with multiple pulses, the contact angles changed insignificantly.

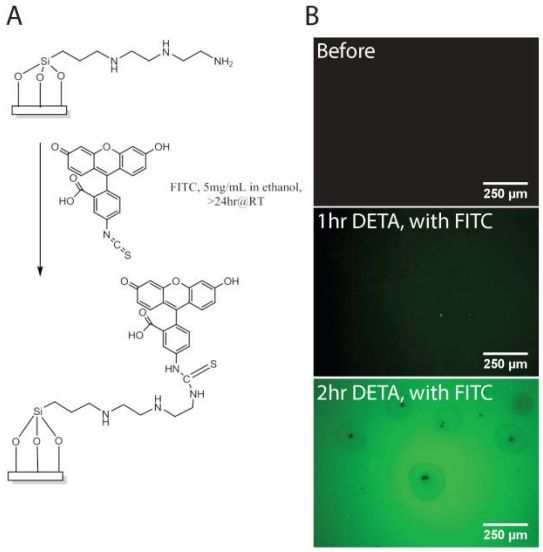

Figure 6: (A) The reaction of FITC linking to DETA. (B) Florescence of FITC binding on DETA-deposited Pyrex wafers. With the intensity of FITC, it was concluded that 2-hour DETA deposition gave better deposition efficiency than 1-hour DETA deposition.

As ODS deposition, we also tested whether multiple pulses could increase DETA deposition efficiency. With both 12 pulses in one hour and 24 pulses in two hours, it was found that the

florescence signal of FITC coating on wafers were similar (Fig. 7). However, comparing with single pulse with two hour deposition, the intensity of florescence was lower. In conclusion, we suggest that two hours deposition with single pulse could give better deposition efficiency.

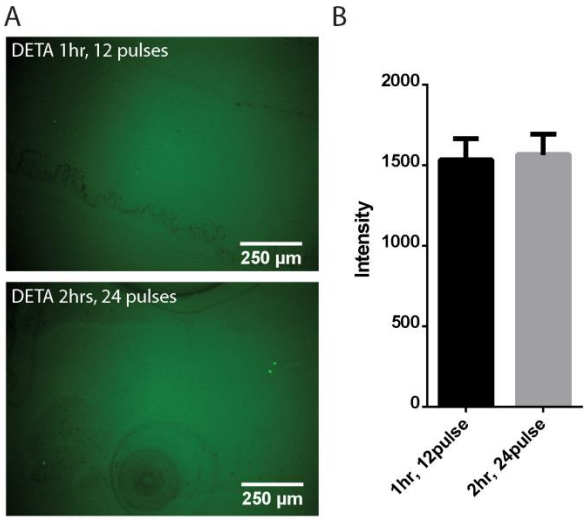

Figure 7: (A) The FITC florescence image of wafers with multi-pulse deposition of DETA. (B) By comparing the intensity of FITC florescence, it was concluded that for multi-pulse deposition, increasing reaction time could not increase deposition efficiency.

Patterning ODS and DETA on Pyrex wafers for cell culture

To deposit both ODS and DETA on Pyrex wafers to direct cell growth, we use photolithography techniques (Fig. 8, detail in Methods and Materials). For the fabrication steps we proposed, the critical steps will be removing ODS by oxygen plasma (Fig. 8E) and the removal of photoresist (Fig. 8G). To test whether oxygen plasma could sufficiently remove organosilane, we used wafers with DETA and FITC coated. The wafers were cleaned with oxygen plasma for 40 seconds and recoated with FITC. It was showed that the florescence signal highly decreased compared with wafers without oxygen plasma treated (Fig. 9A). This indicated that oxygen plasma could be able to remove DETA to prevent FITC binding. Contact angle measurement was also used to evaluate the surface change. After developing and DETA deposition, the contact angle decreased comparing with the one after ODS deposition because the surface became more hydrophilic (Fig. 9B).

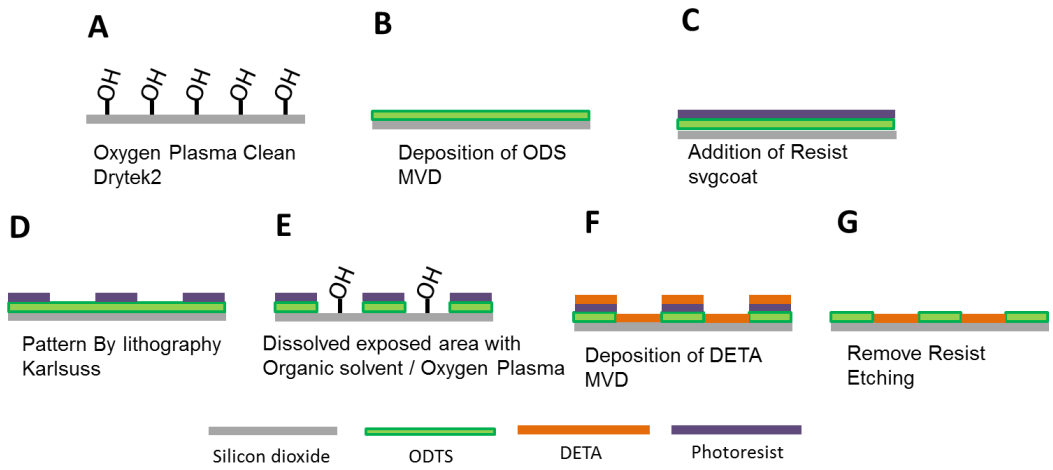

Figure 8: Diagram of making patterned ODS and DETA on Pyrex wafer. (A) Plasma cleaning (B) ODS deposition (C) Photoresist deposition (D) Lithography (E) ODS etched by oxygen plasma (F) DETA deposition (G) Lift off

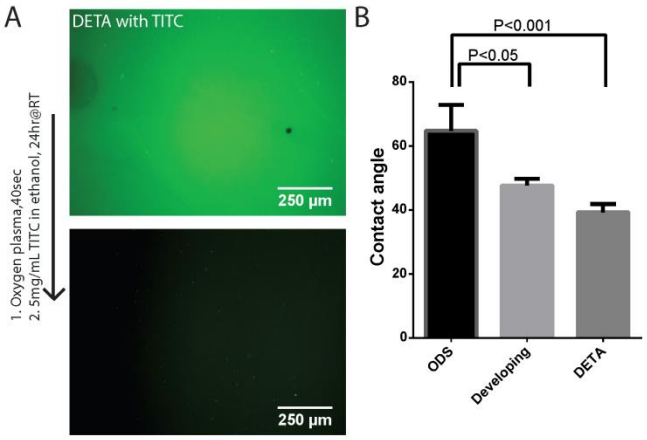

Figure 9: (A) Oxygen plasma remove DETA and thus prevent FITC binding. (B) The change of contact angle showed that the surface composition change during fabrication. The decreasing of contact angle indicated that the surface became more hydrophilic after developing and DETA deposition.

In order to visualize the patterned organosilane, we again used FITC to distinguish between ODS and DETA. We first checked the wafer before lifting off the photoresist with acetone, and we found that the photoresist itself had fluoresced signal under blue light (Fig. 10A). Since after lifting off, the resist will be removed and only ODS will remain, there should be no fluorescence after lifting off and FITC coating. The area without photoresist protection, there will be DETA deposited and will have fluorescence after FITC coating. After lifting off and FITC coating, however, we found that the DETA area showed higher fluorescence signal than ODS area (Fig. 10B). Compared with the signal of photoresist, we concluded that the photoresist was not totally removed so that we could still see the fluorescence of photoresist.

In order to remove photoresist, we first decreased the temperature of reaction chamber to 110°C to prevent the degradation of photoresist. In addition, we use sonication to remove the photoresist when doing lifting off. The results showed that photoresist could be removed by

sonication (Fig. 11). Thus, it was suggested that lower temperature is better for doing lithography for organosilane deposition.

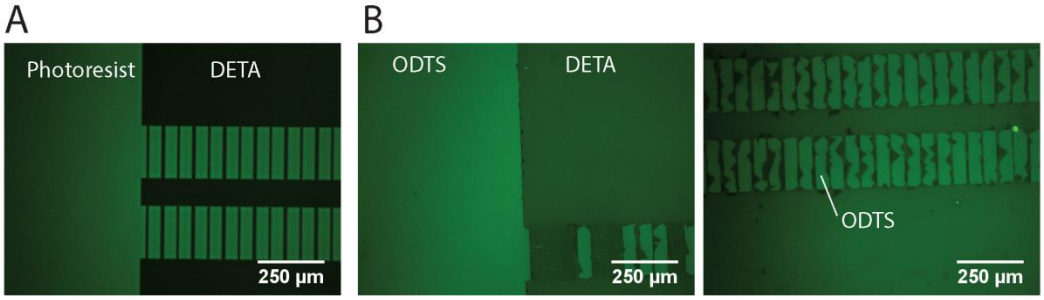

Figure 10: Fluorescence test of patterned organosilane (A) The fluorescence background of photoresist and DETA. (B) FITC coating on the wafer after lifting off photoresist. The high intensity of fluorescence in ODTS area showed that the photoresist was not totally removed.

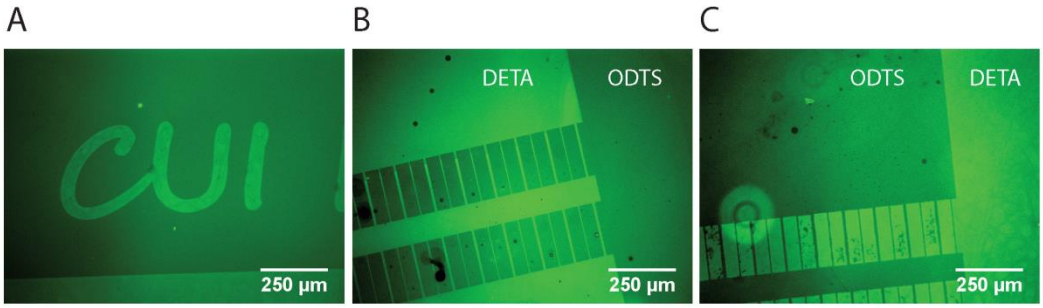

Figure 11: Fluorescence test of patterned organosilane after sonication (A) The "CUI" pattern on the Pyrex wafer. (B) Low fluorescence on the ODTS indicated that the photoresist was removed. (C) With reverse patterning, difference between ODTS and DETA area can also be seen.

Discussion

Mechanism of organosilane deposition

Although we assumed that the deposition efficiency will increase with reaction time. However, the results of ODS deposition showed that deposition efficiency dropped when reaction time was longer than one hour. We suggested that the reason might be the existence of methanol, the side product during the reaction. The organosilane deposition is based on the substitution of methoxy groups of organosilane by the hydroxyl groups on silicon or Pyrex wafers (Fig. 12). During the reaction, the hydroxyl groups will attack the silicon atoms to form new silicon-oxygen covalent bond, and also generate methanol as a side product. Since both ODS and DETA have three methoxy groups, every organosilane molecule can produce up to three methanol molecules during the reaction. In consequence, the concentration of methanol inside the chamber will increase. However, the substitution is reversible, which means that the methanol could attack the silicon atom to break the bond between organosilane and wafer. When the

concentration of methanol is higher, the rate of reverse reaction also becomes higher. Once the reverse reaction rate is higher than the reaction itself, the deposition efficiency will drop.

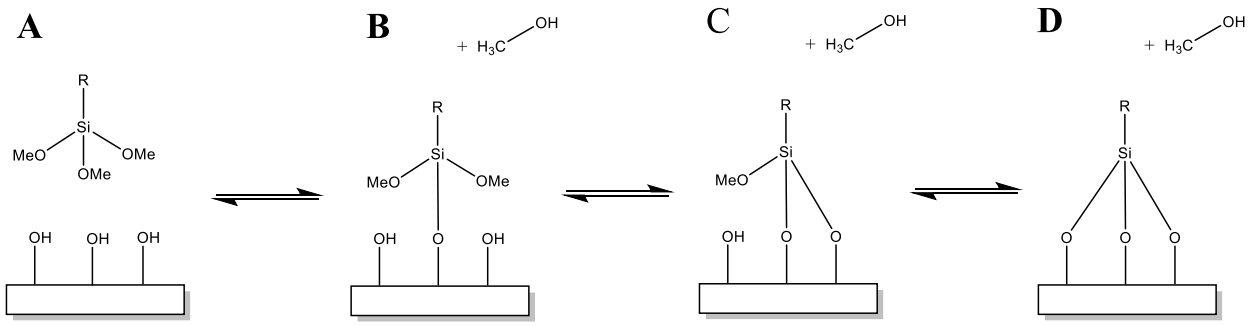

Figure 12: Mechanism of organosilane deposition. (A) The organosilane molecule interacts with surface. (B) One hydroxyl group substitutes one of the methoxy groups of organosilane and releases a methanol molecule. (C) Another hydroxyl group substitutes the second methoxy group and creates second methanol molecule. (D) Finally, the last methoxy group is substituted, totally releases three methanol molecules. All of the reactions are reversible. Methanol could attack the silicon to form methoxy group.

With short reaction time, the forward reaction is dominated. Thus, the deposition efficiency increases with longer reaction time. However, once the reaction time is long enough to generate enough methanol molecules, the reverse reaction will become dominated and thus the deposition efficiency starts to decrease. This reaction will eventually reach to equilibrium, which means the forward reaction rate is equal to the reverse reaction rate. Thus, the deposition efficiency will eventually become independent with reaction time.

Conclusion and future work

We developed methods of depositing organosilane on silicon and Pyrex wafers by MVD. By measuring contact angle and coating FITC, the deposition efficiency of ODS and DETA could be quantified, respectively. In the course of this study, it was determine that long deposition time does not guarantee higher ODS deposition efficiency. According to our results, it was indicated that the presence of the methanol could reverse the silination reaction. This phenomenon, however, was not observed in DETA deposition. To fabricate a template for directing neuron cell growth, ODS and DETA were patterned by photolithography. With their different affinity of binding FITC, fabricated patterns could be visualized by fluoresce microscopy.

We proposed that future studies should concentrate on characterizing the activated site by FTIR and other adequate instrument. Accomplish this task would give a better representation of

deposition efficiency. Ultimately, we would like to apply this technique to create artificial neuronal circuits for the purpose of studying neural networks electrical activities.

References

(1) Palyvoda, O.; Chen, C.-C.; Auner, G. W. *Biosens. Bioelectron.* **2007**, *22*, 2346–2350.
(2) Yamaguchi, M.; Ikeda, K.; Suzuki, M.; Kiyohara, A.; Kudoh, S. N.; Shimizu, K.; Taira, T.; Ito, D.; Uchida, T.; Gohara, K. *Langmuir* **2011**, *27*, 12521–12532.
(3) Ressier, L.; Martin, C.; Viallet, B.; Grisolia, J.; Peyrade, J.-P. *J. Vac. Sci. Technol. B Microelectron. Nanom. Struct.* **2007**, *25*, 17.
(4) Yang, Y.; Bittner, A. M.; Baldelli, S.; Kern, K. **2008**, *516*, 3948–3956.
(5) Glass, N. R.; Tjeung, R.; Chan, P.; Yeo, L. Y.; Friend, J. R. *Biomicrofluidics* **2011**, *5*, 036501, 7 pp.
(6) Wang, M.; Liechti, K. M.; Wang, Q.; White, J. M. *Langmuir* **2005**, *21*, 1848–1857.
(7) Li, N.; Ho, C.-M. *Lab Chip* **2008**, *8*, 2105–2112.
(8) Sandhyarani, N.; Pradeep, T. **2001**, *338*, 33–36.
(9) Gunda, N. S. K.; Singh, M.; Norman, L.; Kaur, K.; Mitra, S. K. *Appl. Surf. Sci.* **2014**, *305*, 522–530.
(10) Schreiber, F. *Prog. Surf. Sci.* **2000**, *65*, 151–257.
(11) Pallandre, A.; Glinel, K.; Jonas, A. M.; Nysten, B. *Nano Lett.* **2004**, *4*, 365–371.
(12) Zhang, F.; Sautter, K.; Larsen, A. M.; Findley, D. A.; Davis, R. C.; Samha, H.; Linford, M. R. **2010**, *26*, 14648–14654.
(13) Prasittichai, C.; Zhou, H.; Bent, S. F. *ACS Appl. Mater. Interfaces* **2013**, *5*, 13391–13396.
(14) Zhou, H.; Toney, M. F.; Bent, S. F. *Macromolecules* **2013**, *46*, 5638–5643.
(15) Loscutoff, P. W.; Zhou, H.; Clendenning, S. B.; Bent, S. F. **2010**, *4*, 331–341.
(16) Yamamoto, H.; Okano, K.; Demura, T.; Hosokawa, Y.; Masuhara, H.; Tanii, T.; Nakamura, S. *Appl. Phys. Lett.* **2011**, *99*, 163701.
(17) Sugimura, H.; Hozumi, A.; Kameyama, T.; Takai, O. *Surf. Interface Anal.* **2002**, *34*, 550–554.
(18) Färm, E.; Kemell, M.; Ritala, M.; Leskelä, M. *Chem. Vap. Depos.* **2006**, *12*, 415–417.
(19) Liu, J.; Rumsey, J. W.; Das, M.; Molnar, P.; Gregory, C.; Riedel, L.; Hickman, J. J. *In Vitro Cell. Dev. Biol. Anim.* **2008**, *44*, 162–168.